

The residue at position 5 of the N-terminal region of Src and Fyn modulates their myristoylation, palmitoylation, and membrane interactions

Efrat Gottlieb-Abraham^a, Orit Gutman^a, Govind M. Pai^b, Ignacio Rubio^b, and Yoav I. Henis^{a,*}

^aDepartment of Neurobiology, George S. Wise Faculty of Life Sciences, Tel Aviv University, Tel Aviv 69978, Israel;

^bInstitute of Molecular Cell Biology, Center for Molecular Biomedicine, University Hospital, Jena 07745, Germany

ABSTRACT The interactions of Src family kinases (SFKs) with the plasma membrane are crucial for their activity. They depend on their fatty-acylated N-termini, containing N-myristate and either a polybasic cluster (in Src) or palmitoylation sites (e.g., Fyn). To investigate the roles of these moieties in SFK membrane association, we used fluorescence recovery after photobleaching beam-size analysis to study the membrane interactions of c-Src-GFP (green fluorescent protein) or Fyn-GFP fatty-acylation mutants. Our studies showed for the first time that the membrane association of Fyn is more stable than that of Src, an effect lost in a Fyn mutant lacking the palmitoylation sites. Unexpectedly, Src-S3C/S6C (containing cysteines at positions 3/6, which are palmitoylated in Fyn) exhibited fast cytoplasmic diffusion insensitive to palmitoylation inhibitors, suggesting defective fatty acylation. Further replacement of the charged Lys-5 by neutral Gln to resemble Fyn (Src-S3C/S6C/K5Q) restored Fyn-like membrane interactions, indicating that Lys-5 in the context of Src-S3C/S6C interferes with its myristoylation/palmitoylation. This was validated by direct myristoylation and palmitoylation studies, which indicated that the residue at position 5 regulates the membrane interactions of Src versus Fyn. Moreover, the palmitoylation levels correlated with targeting to detergent-resistant membranes (rafts) and to caveolin-1. Palmitoylation-dependent preferential containment of Fyn in rafts may contribute to its lower transformation potential.

Monitoring Editor

Keith E. Mostov
University of California, San Francisco

Received: Aug 31, 2016

Revised: Oct 3, 2016

Accepted: Oct 5, 2016

INTRODUCTION

The Src family kinases (SFKs) are nonreceptor tyrosine kinases that play key roles in a variety of cellular processes, including differentiation, proliferation, and migration, and affect the metastatic potential of tumor cells (Abram and Courtneidge, 2000; Irby and Yeatman, 2000; Martin, 2001; Frame, 2004; Ingley, 2008). All SFKs

share a similar domain structure, composed of a catalytic domain (SH1) followed by a short unique linker region, SH2 and SH3 protein interaction modules, and an N-terminal membrane anchor (SH4) (Brown and Cooper, 1996; Resh, 1999; Martin, 2001; Boggon and Eck, 2004). The SH3 and SH2 domains are required both for SFK autoinhibition (forming a folded, inactive conformation by binding to polyproline residues and to a phosphotyrosine [pTyr] residue at the SFK C-terminal region, respectively), and for the targeting of activated SFKs to protein phosphorylation substrates (Sicheri *et al.*, 1997; Xu *et al.*, 1997; Frame, 2004; Shvartsman *et al.*, 2007; Oneyama *et al.*, 2008). Recently we have shown that tyrosine phosphorylation of cell-surface proteins by c-Src (Src) directs the binding of the SH2 domain of activated Src to pTyr sites on these proteins, regulating Src association with and localization in the plasma membrane (Shvartsman *et al.*, 2007). In the case of caveolin-1 (Cav-1), this led to accumulation of activated Src in focal adhesions (Gottlieb-Abraham *et al.*, 2013).

The membrane association and intracellular distribution of SFKs depend on their N-terminal membrane anchor (Brown and Cooper, 1996; Resh, 1999, 2006; Sandilands *et al.*, 2007). The

This article was published online ahead of print in MBoC in Press (<http://www.molbiolcell.org/cgi/doi/10.1091/mbc.E16-08-0622>) on October 12, 2016.

*Address correspondence to: Yoav I. Henis (henis@post.tau.ac.il)

Abbreviations used: 2BP, 2-bromopalmitate; Cav-1, caveolin-1; Cbp, Csk-binding protein; *D*, lateral diffusion coefficient; DRM, detergent-resistant membrane; FCS, fetal calf serum; FRAP, fluorescence recovery after photobleaching; GFP, green fluorescent protein; HBSS, Hank's balanced salts solution; mRFP, monomeric red fluorescent protein; NMT, N-myristoyl transferase; pCav-1, pY14-Cav-1; pTyr, phosphotyrosine; *R_f*, mobile fraction; SFK, Src family kinase; τ , characteristic fluorescence recovery time; WT, wild type.

© 2016 Gottlieb-Abraham *et al.* This article is distributed by The American Society for Cell Biology under license from the author(s). Two months after publication it is available to the public under an Attribution-Noncommercial-Share Alike 3.0 Unported Creative Commons License (<http://creativecommons.org/licenses/by-nc-sa/3.0>).

"ASCB®," "The American Society for Cell Biology®," and "Molecular Biology of the Cell®" are registered trademarks of The American Society for Cell Biology.

N-myristoylation site at the N-terminus (Gly-2), which is common to all SFKs (Resh, 1994), is myristoylated cotranslationally by N-myristoyl transferase (NMT; Farazi et al., 2001), which recognizes specific sequence motifs at the N-terminus of the substrate proteins, a major one of which is located at positions 2–7 (which become 1–6 after the initiating methionine is removed during translation, leaving the myristoylated glycine as the N-terminal amino acid; Maurer-Stroh et al., 2002). This myristoylation is necessary but not sufficient for their membrane anchorage, which requires a second signal. In most SFKs (e.g., Fyn and Yes), the second signal is provided by one or two palmitoylation sites at the N-terminal region; these are absent in Src, which instead contains in this region a polybasic cluster interacting with the negatively charged phospholipids in the plasma membrane inner leaflet (Sigal et al., 1994; McLaughlin and Aderem, 1995; Resh, 2006). Of note, in palmitoylation-capable SFKs, myristoylation is a prerequisite for the ensuing palmitoylation (Koegele et al., 1994). The differences in the membrane anchor may be relevant to the targeting of different SFKs to distinct plasma membrane domains, since the palmitoylation of membrane-associated proteins was shown to play an important role in their targeting to cholesterol-enriched membrane assemblies termed lipid rafts (Simons and Toomre, 2000; Hancock, 2006; Jacobson et al., 2007; Eisenberg et al., 2013; Parton and del Pozo, 2013). Resembling the preferential raft localization of the palmitoylated H-Ras and N-Ras, but not the nonpalmitoylated K-Ras (which is anchored in the membrane via a C-terminal farnesylated cysteine and a polybasic cluster; Hancock, 2003; Henis et al., 2009; Eisenberg et al., 2013), palmitoylated SFKs were reported to display higher affinity to detergent-resistant membranes (DRMs) and caveolae than the nonpalmitoylated Src (Shenoy-Scaria et al., 1994; Melkonian et al., 1999; Resh, 1999; Oneyama et al., 2009). This phenomenon can have important implications for SFK signaling, since preferential targeting of individual SFKs to raft domains may limit their transforming potential (Oneyama et al., 2008, 2009; Cai et al., 2011; Gottlieb-Abraham et al., 2013).

In spite of the importance of understanding the relationships between the different N-terminal SFK anchor signals (myristoylation, palmitoylation, and positive charge), their potential interdependence and concerted ability to regulate the membrane interactions and raft domain targeting of different SFKs remained unclear. Here we investigated these issues by combining biophysical studies in live cells with biochemical studies to explore the interactions of wild-type (WT) and structural mutants of Src and Fyn with the plasma membrane and with lipid rafts. Our findings show for the first time that palmitoylation at the N-terminal anchor region stabilizes the interactions of the above unactivated SFKs with the plasma membrane. In line with earlier reports, it also targets them to raft domains. The palmitoylation is intertwined with initial myristoylation, and we show that both are modulated by the residue at position 5 (charged lysine vs. neutral glutamine) and the neighboring residues at positions 3 and 6 (mainly the latter). Thus a novel conclusion is that the residue at position 5 modulates the membrane interactions of Src vs. Fyn. For constitutively active Src and Fyn, the membrane association is similarly strengthened by virtue of dynamic interactions of the open conformation with membrane-associated pTyr protein targets. The preferential targeting of palmitoylated SFKs to rafts and/or caveolae may limit their ability to activate non-raft transforming pathways.

RESULTS

Palmitoylation stabilizes Src/Fyn membrane association

To explore the dependence of the membrane interactions of Src and Fyn on their N-terminal fatty-acylated membrane anchors, we

Src/Fyn construct	N-terminal sequence
Src-WT	M G S S K S K P K D P S Q R R R
Src-G2A	M A S S K S K P K D P S Q R R R
Src-S3C/S6C	M G C S K C K P K D P S Q R R R
Src-S3C/S6C/K5Q	M G C S Q C K P K D P S Q R R R
Fyn-WT	M G C V Q C K D K E A T K L T E
Fyn-C3S/C6S	M G S V Q S K D K E A T K L T E

The mutated amino acids are shadowed. All constructs were GFP-tagged (see *Materials and Methods*).

TABLE 1: Schematic representation of the N-terminal amino acid sequence of Src and Fyn mutants used in the current studies.

used human Fyn GFP-tagged constructs (Fyn-WT, and Fyn-C3S/C6S lacking the two palmitoylation sites), Src-WT, and a Src mutant imitating the N-terminal anchor of Fyn by incorporation of two potential palmitoylation sites (Src-S3C/S6C). The constructs are depicted in Table 1 and described under *Plasmids* in *Materials and Methods*. These proteins were expressed in COS7 cells, which were subjected to fluorescence recovery after photobleaching (FRAP) beam-size analysis. Typical results are shown in Figure 1, A and B, while averaged data derived from experiments on multiple cells are depicted in Figure 1, C and D. The FRAP beam-size analysis measures the interactions of nonintegral membrane proteins with the plasma membrane (Henis et al., 2006; Shvartsman et al., 2007). It uses two laser beam sizes, generated by focusing the laser beam through a 63x (smaller Gaussian radius, ω) or a 40x (larger ω) objective (Henis et al., 2006). The ratio between the illuminated areas, $\omega^2(40x)/\omega^2(63x)$, was 2.28 in the current experiments. For FRAP by lateral diffusion, τ (the characteristic fluorescence recovery time) is the characteristic diffusion time τ_D , which is proportional to the area bleached by the focused laser beam ($\tau_D = \omega^2/4D$, where D is the lateral diffusion coefficient). This occurs because when molecules diffuse with a defined diffusion coefficient, enlarging the diffusion area by, for example, 2 will result in a similar increase in the diffusion time, since the molecules diffuse at the same rate but have to cover twice the distance. Therefore, when the recovery occurs by lateral diffusion, the $\tau(40x)/\tau(63x)$ ratio should be equal to the beam-size ratio (2.28). On the other hand, a τ ratio of 1 (no dependence on the bleached area size) is indicative of FRAP by exchange between membrane-associated and cytoplasmic pools of the fluorescent protein. This situation arises because for recovery by exchange, τ reflects the chemical relaxation time rather than diffusion time, and the chemical relaxation time is independent of the dimensions of the bleached area. Therefore, in this case, τ is the characteristic exchange time τ_{ex} . τ ratios between 2.28 and 1 suggest a mixed recovery mode (Henis et al., 2006; Shvartsman et al., 2007).

The results depicted in Figure 1 demonstrate, for the first time, significant differences between the membrane interaction dynamics of Fyn and Src. Fyn-WT-GFP interacted with the plasma membrane more stably than Src-WT-GFP, as attested by its $\tau(40x)/\tau(63x)$ ratio, which is much closer (2 vs. 1.4 obtained for Src-WT) to the 2.28 value typical of recovery by pure lateral diffusion. This suggests a much lower contribution of membrane-cytoplasm exchange to the FRAP of Fyn-WT. Accordingly, the FRAP rate of Fyn-WT is also slower than that of Src-WT (Figure 1, C and D). Owing to the contribution of exchange to the FRAP process, accurate calculation of D is not possible, but it can be estimated from the $\tau(63x)$ values, since the smaller bleach area reduces τ_D but not τ_{ex} , leading to a higher contribution of lateral diffusion (Shvartsman et al., 2007).

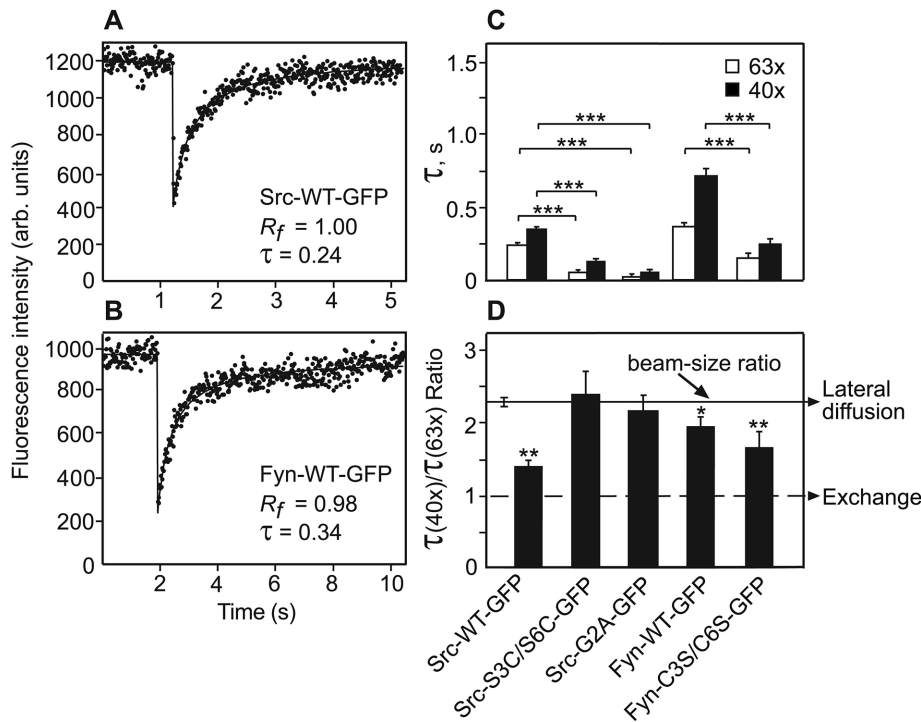


FIGURE 1: FRAP beam-size analysis of the membrane interactions of Src and Fyn palmitoylation mutants. COS7 cells were transfected with expression vectors encoding the indicated GFP-tagged Src or Fyn proteins. FRAP experiments were conducted 24 h posttransfection at 22°C. (A, B) Typical FRAP curves of Src-WT-GFP and Fyn-WT-GFP. The curves shown were obtained using the 63x objective. Solid lines show the best fit of a nonlinear regression analysis (see *Materials and Methods*), with the resulting τ and mobile fraction (R_f) values. Note the different time scales in the two panels. (C, D) Average τ and $\tau(40x)/\tau(63x)$ (τ ratio) values derived from multiple FRAP beam-size analysis experiments. The studies used the 63x and 40x objectives and were conducted as described under *Materials and Methods*. These objectives yield a 2.28 ± 0.17 beam-size ratio (solid line in panel D), which is therefore the τ ratio expected for FRAP by lateral diffusion. A τ ratio of 1 (dashed lines) is expected for recovery by exchange (Henis *et al.*, 2006). Bars are mean \pm SEM of 30–60 measurements in each case. The R_f values were above 0.95 in all cases and are therefore not shown. (C) τ values. Asterisks indicate significant differences between the $\tau(63x)$ or $\tau(40x)$ values of Src- or Fyn-WT and their mutants, comparing the τ values measured with the same beam size (***, $p < 10^{-11}$; Student's *t* test). (D) $\tau(40x)/\tau(63x)$ ratios. Bootstrap analysis, which is better-suited for comparison between ratios, shows that the τ ratios of Src-WT and Fyn-C3S/C6S (both of which lack palmitoylation sites but undergo myristoylation) are very different from the 2.28 ratio characterizing recovery by lateral diffusion, indicating a significant contribution of exchange to the FRAP (**, $p < 10^{-4}$). The τ ratio measured for Fyn-WT was also significantly lower than 2.28, albeit with lower significance (*, $p < 10^{-2}$). Finally, Src-S3C/S6C-GFP and Src-G2A-GFP yielded fast recovery indicative of mainly cytoplasmic diffusion (C); the τ ratios measured for these mutants were also in line with cytoplasmic diffusion (D), as they were similar to the beam-size ratio used for the bleaching (Wolfenson *et al.*, 2009).

The values thus obtained for *D* were 0.62 and 0.41 $\mu\text{m}^2/\text{s}$ for Src-WT-GFP (in line with earlier findings; Shvartsman *et al.*, 2007) and Fyn-WT-GFP, respectively. The above differences between the FRAP parameters of Fyn-WT and Src-WT appear to be due to the palmitoylation sites present only in the first, as demonstrated by the shift of the Fyn-C3S/C6S mutant (lacking the palmitoylation sites) to a lower $\tau(40x)/\tau(63x)$ ratio, which suggests an increased contribution of exchange to the FRAP mechanism, accompanied by a two-fold-faster FRAP recovery rate. Of note, unexpected FRAP beam-size analysis results were obtained for Src-S3C/S6C-GFP, a Src mutant considered to imitate Fyn due to mutation of the Ser residues at positions 3 and 6 to Cys, generating potential palmitoylation sites as in Fyn (Sandilands *et al.*, 2007). Surprisingly, this mutant exhibited very fast FRAP recovery (much faster than that of either Src-WT or Fyn-WT; Figure 1), close to the range of cytoplasmic

protein diffusion (Wolfenson *et al.*, 2009), suggesting that this mutant may have a largely reduced capability to undergo fatty acylation. This interpretation is in line with the finding that the τ ratio obtained for this mutant was similar to the beam-size ratio (2.28), as expected for recovery by pure diffusion in the cytoplasm. As we demonstrated earlier (Wolfenson *et al.*, 2009), FRAP for diffusion in the cytoplasm is a projection of the diffusion in the three-dimensional space to two dimensions and obeys the same rules as the latter. Indeed, a Src mutant known to be cytoplasmic due to the absence of the myristoylation site (Src-G2A-GFP; Newsome *et al.*, 2006; Patwardhan and Resh, 2010) showed the same phenomenon and exhibited fast cytoplasmic diffusion (about twofold faster than that of Src-S3C/S6C, most likely since Src-G2A is not capable of undergoing even a low level fatty acylation; see Figure 5 later in this article) and a τ ratio not significantly different from 2.28 (Figure 1). These findings suggest that the fatty-acylation of Src-S3C/S6C may be defective, resulting in very weak interactions with the plasma membrane. In line with this notion, inhibition by 2-bromopalmitate (2BP), a known inhibitor of protein palmitoylation (Ahearn *et al.*, 2011), shifted the FRAP dynamics of Fyn-WT to values resembling those of Src-WT (Figure 2; compare the 2BP-treated Fyn-WT results to those of untreated Src-WT in Figure 1), but had no effect on Src-S3C/S6C dynamics (Figure 2). This indicates that palmitoylation does not significantly contribute to the interactions of the latter mutant with the plasma membrane.

Src/Fyn fatty acylation and membrane interactions are modulated by the residue at position 5

The above findings suggest that although Src-S3C/S6C was expected to be a “Fyn-like” Src mutant and to have additional membrane interactions due to its potential palmitoylation sites, it fails to bind effectively to the membrane. We hypothesized that this may occur due to differences between Src and Fyn in the lipid anchor region, which interfere with effective myristoylation of the Src-S3C/S6C mutant, and therefore also inhibit further palmitoylation. Lys-5, which is part of the polybasic cluster in Src, is the closest to the N-terminus and the myristoylation site (Gly-2), and is located right between Ser-6 and Ser-3, which are replaced by Cys residues in Fyn and in the Src-S3C/S6C mutant. Moreover, the positively charged Lys-5 is replaced in Fyn by a neutral Gln5 residue. Therefore we proceeded to explore whether replacement of Lys-5 by Gln in the Src-S3C/S6C mutant affects its membrane targeting. To this end, we prepared the triple Src mutant Src-S3C/S6C/K5Q-GFP and expressed it in COS7 cells that were subjected to FRAP beam-size analysis, both without and with 2BP treatment. As shown in Figure 3, replacing Lys-5 by Gln in Src-S3C/S6C reverted

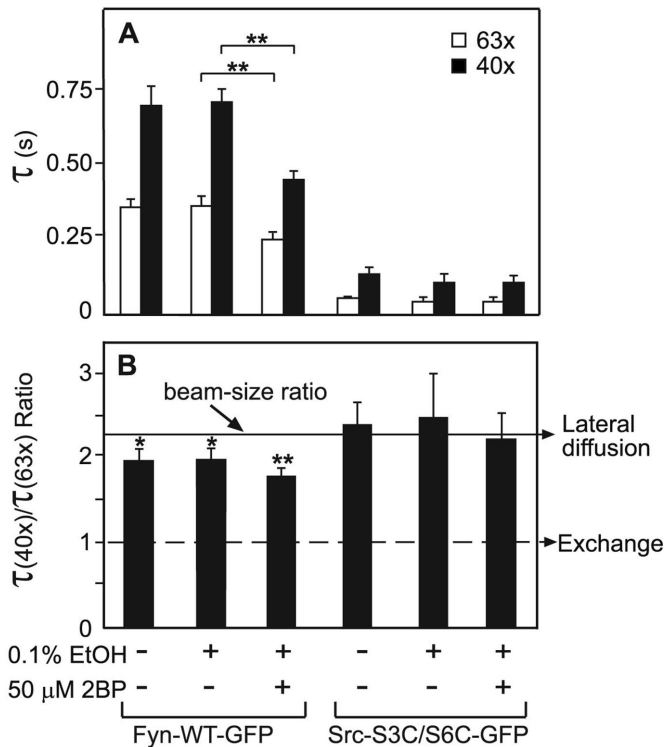


FIGURE 2: The interactions of Src-S3C/S6C with the plasma membrane are insensitive to inhibition of palmitoylation. COS7 cells were transfected with vectors encoding Src-S3C/S6C-GFP or Fyn-WT-GFP. After 24 h, FRAP beam-size analysis studies were conducted with the 63x and 40x objectives as in Figure 1, either on untreated cells or on cells incubated with 50 μM of the palmitoylation inhibitor 2BP (or with vehicle, 0.1% ethanol), adding the drug or the vehicle at 6 h posttransfection. Bars are means ± SEM of 30–60 measurements. (A) τ values. Treatment with 2BP reduced significantly (**, $p < 10^{-5}$, Student's t test) the recovery times of Fyn-WT, but not of Src-S3C/S6C. (B) τ(40x)/τ(63x) ratios. Bootstrap analysis shows that the τ ratio of Fyn-WT is only mildly below the 2.28 value expected for lateral diffusion (*, $p < 10^{-2}$), but is further reduced in the presence of 2BP to become more significantly below this value (**, $p < 10^{-4}$). On the other hand, no significant effects of 2BP were observed on the τ ratios of Src-S3C/S6C, which were indistinguishable from the 2.28 value (pure diffusion) in all cases.

its FRAP rates as measured with both objectives from the very low τ values measured for Src-S3C/S6C to values resembling those of Fyn-WT (which undergoes palmitoylation), accompanied by a τ ratio very close to 2.28, as expected for stable membrane interactions. These results strongly suggest that the triple Src mutant imitates Fyn in its association with the plasma membrane, in line with effective palmitoylation of its N-terminal Cys residues. This notion gains further support from the sensitivity to 2BP exhibited by the Src-S3C/S6C/K5Q mutant (Figure 3); treatment by the palmitoylation inhibitor shifted the τ values of this mutant to significantly lower values, which were closer to the values measured for Src than for Fyn (see Figure 1). These results are in accord with inhibition of palmitoylation of Src-S3C/S6C/K5Q by 2BP.

Our earlier studies have shown that the free SH2 domain of activated, open-conformation Src binds dynamically to pTyr-membrane protein targets, resulting in stronger membrane association than that conferred on the folded conformation by the N-terminal anchor (Shvartsman *et al.*, 2007). Therefore it is expected that differences in the fatty acylation of the N-terminal region of Src, Fyn

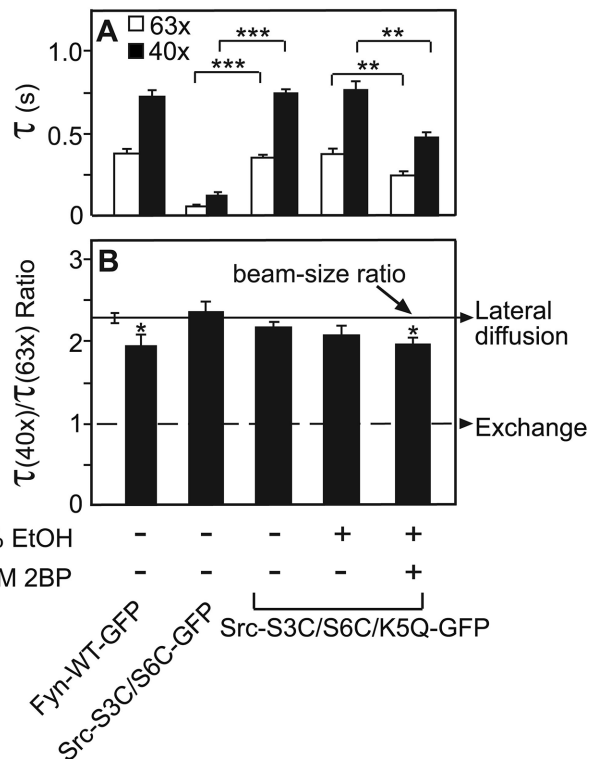


FIGURE 3: Src-S3C/S6C/K5Q displays Fyn-like membrane interactions that are sensitive to inhibition of palmitoylation. Cells transfected with expression vectors for Src-S3C/S6C/K5Q-GFP, Src-S3C/S6C-GFP, or Fyn-WT-GFP were subjected to FRAP beam-size analysis experiments with the 63x and 40x objectives as described in Figure 1. In some experiments, treatment with 2BP or with vehicle (0.1% ethanol) was carried out as described in Figure 2. Bars are means ± SEM of 30–60 measurements. (A) τ values. Replacement of Lys-5 by Gln in Src-S3C/S6C dramatically increased its τ values, as predicted to occur upon conferment of association with the plasma membrane (***, $p < 10^{-11}$; Student's t test). These values became similar to those of Fyn-WT-GFP. Moreover, treatment with 2BP significantly reduced the τ values of Src-S3C/S6C/K5Q, suggesting that palmitoylation contributes to its membrane interactions (**, $p < 10^{-5}$). (B) τ(40x)/τ(63x) ratios. Bootstrap analysis shows that all the τ ratios are close to the values expected for a major contribution to the FRAP by diffusion. A significant deviation from the 2.28 beam-size ratio, attesting to a measurable contribution by exchange, is observed for Fyn-WT and for 2BP-treated Src-S3C/S6C/K5Q (*, $p < 10^{-2}$).

and their mutants would disappear or become significantly weaker in the corresponding constitutively active mutants. As shown in Figure 4, this prediction was met for constitutively active Src (Src-Y527F), constitutively active Fyn (Fyn-Y531F), and the constitutively active version of the Fyn-like Src mutant Src-S3C/S6C/K5Q/Y527F. All these constitutively active mutants exhibited τ values significantly slower than those of their WT counterparts, with τ ratios close to the value expected for lateral diffusion. This finding is in accord with dynamic interactions of the activated SFKs with slower-diffusing transmembrane proteins (Shvartsman *et al.*, 2007). Of note, adding the Y527F constitutively activating mutation to the mainly cytoplasmic Src-S3C/S6C did not increase significantly its membrane interactions, suggesting for the first time that the activated SFK has to come into close proximity with the membrane prior to the binding to pTyr membrane protein targets via its SH2 domain.

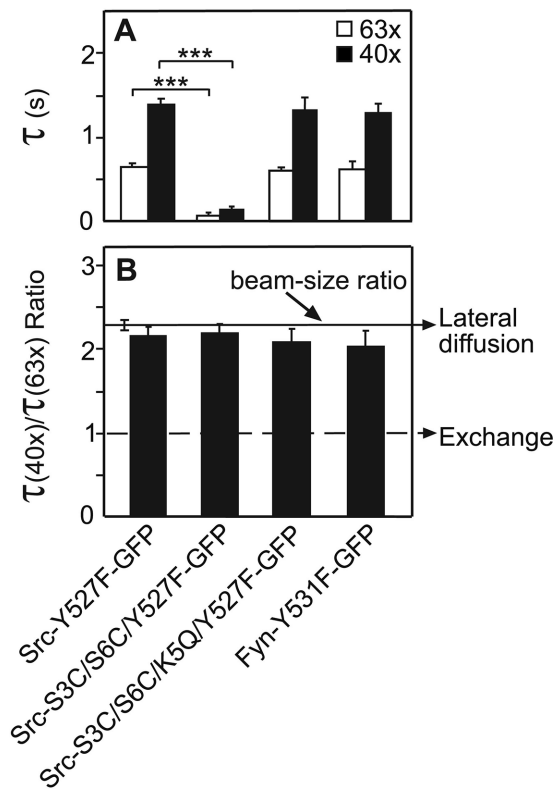


FIGURE 4: FRAP beam-size analysis of the membrane interactions of activated Src and Fyn mutants. Cells transfected with vectors encoding the indicated proteins, each containing a constitutively activating mutation (Y527F in Src, Y531F in Fyn), were subjected to FRAP beam-size analysis as in Figure 1. Bars, means \pm SEM of 30–60 measurements. (A) τ values. Asterisks indicate significant differences between the $\tau(63x)$ or $\tau(40x)$ values of the pairs indicated by the brackets, comparing τ values measured with the same beam size ($***, p < 10^{-11}$; Student's *t* test). (B) $\tau(40x)/\tau(63x)$ ratios. All τ ratios were not significantly different from the 2.28 beam-size ratio (the value expected for recovery by diffusion) and were not significantly different from each other.

To obtain a biochemical corollary to the biophysical studies, we analyzed the palmitate and myristate content of the unactivated Src-GFP and Fyn-GFP proteins (WT and mutants). Cells transfected with the indicated expression vectors were metabolically labeled by [3 H] palmitate or [3 H]myristate, following an earlier-described protocol (Song *et al.*, 2013; see *Materials and Methods*). The cell lysates were subjected to immunoprecipitation with anti-GFP antibodies. A fraction of each immunoprecipitated sample served to determine the Src-GFP or Fyn-GFP levels by Western blotting, while the major portions were run on SDS–PAGE and subjected to determination of the levels of [3 H]myristate or [3 H]palmitate by fluorography. Figure 5, A and B, depicts representative fluorography and Western blot results of a typical experiment, and the average data from all experiments are shown in panels C and D. To account for variable Src/Fyn protein expression levels, we always built the ratio of the fluorographic signal to total protein as measured by immunoblotting. It should be noted that a low but detectable level of palmitate was measured in Src (panel B, lane 2), although Src lacks palmitoylation sites. This false-positive signal may result from transfer of [3 H] by exchange from [3 H]palmitate to myristate during the long fluorography exposures or could be due to metabolic interconversion of palmitate and

myristate during the 12-h metabolic labeling period. The latter notion is supported by the absence of the background signal in Src-G2A, which lacks Gly-2 (the myristoylation target). Indeed, the G/A mutation (Src-G2A-GFP) eliminated both the myristoylation and the background palmitoylation. At the same time, the fact that strongly myristoylated variants other than Src, such as Fyn-C3S/C6S, showed only negligible [3 H]-signal in palmitate-labeled cells (Figure 5, right panels) illustrates the extent and impact of metabolic palmitate-to-myristate interconversion is low, as it is negligible for this mutant. Overall the results of the biochemical experiments with all Src and Fyn mutants were in excellent correlation with those of the biophysical studies: 1) Src-S3C/S6C exhibited strongly reduced myristoylation (5.2-fold lower relative to Src) and palmitoylation (approximately threefold lower compared with Fyn), in accord with the biophysical data, which showed the majority of the population of this mutant to behave as a cytoplasmic protein. The τ values measured for this mutant were approximately twofold slower than those measured for Src-G2A, in line with a small but detectable contribution of a minor population of fatty-acylated Src-S3C/S6C molecules to the FRAP. 2) Replacing Lys-5 by Gln in this mutant restored concomitantly the myristoylation and palmitoylation of the triple Src-S3C/S6C/K5Q mutant to levels resembling those of the WT proteins (myristoylation in Src, and palmitoylation in Fyn). This suggests that the charged Lys-5 can be tolerated for recognition by NMT as long as Ser is present at position 6 (as in Src), but not when it is replaced by Cys (see *Discussion*). These results are in complete agreement with the biophysical data, where the K5Q mutation reinstated the interactions with the plasma membrane, and are in line with the notion that palmitoylation depends on an initial myristoylation of the protein. 3) In Fyn, the C3S/C6S double mutation increased the level of myristoylation, which was originally lower than that observed in Src, to a level similar to that of Src. Again, this is in accord with the demonstration that Ser/Thr at position 6 of Src are preferred for myristoylation by NMT (Maurer-Stroh *et al.*, 2002). The palmitoylation of this mutant is dramatically reduced, in line with the mutation of its palmitoylation sites.

Palmitoylation enhances the association of Src/Fyn with lipid rafts and Cav-1

Dual fatty acylation, and especially palmitoylation of at least one site, was shown to target membrane-associated proteins to DRMs and caveolae (Melkonian *et al.*, 1999; Hancock, 2003; Henis *et al.*, 2009; Eisenberg *et al.*, 2013). This includes SFKs (Shenoy-Scaria *et al.*, 1994; Resh, 1999; Suzuki *et al.*, 2007; Oneyama *et al.*, 2008, 2009), whose differential confinement to raft domains was proposed to regulate their activity with respect to transformation (Oneyama *et al.*, 2008, 2009; Cai *et al.*, 2011). Therefore we investigated the association of the different Src-GFP and Fyn-GFP mutants with DRMs. As shown in Figure 6, the distribution of the SFKs and their mutants to DRM and non-DRM fractions was in good correlation with both the biophysical studies and the biochemical experiments on the fatty-acylation levels. Thus Src-WT (lacking palmitoylation sites) and Src-G2A (which is mainly cytoplasmic due to the loss of the myristoylation site) appeared almost only in non-DRM fractions; the Src-S3C/S6C mutant, which has very weak membrane interactions in spite of adding the potential palmitoylation sites due to the strong reduction in its myristoylation, showed only a small increase in the distribution to DRMs. On the other hand, adding the K5Q mutation (the Src-S3C/S6C/K5Q mutant), which rescues the myristoylation and therefore also the ensuing palmitoylation (Figure 5), led to a strong increase in its distribution to DRMs, resembling that of the palmitoylated Fyn-WT. Finally, removal of the palmitoylation

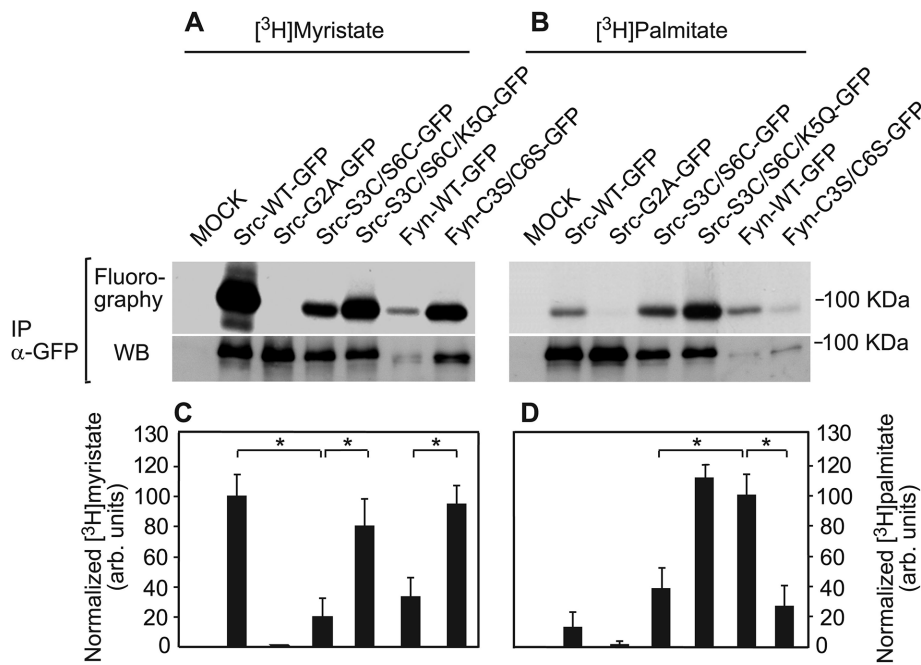


FIGURE 5: Myristoylation and palmitoylation of Src and Fyn mutants correlate with their membrane interactions. COS7 cells expressing the indicated Src-GFP or Fyn-GFP proteins were metabolically labeled with [³H]myristate or [³H]palmitate as described under *Materials and Methods*. The Src-GFP or Fyn-GFP proteins were immunoprecipitated using sheep anti-GFP (α -GFP) antibodies and protein A/GammaBind-sepharose and subjected to fluorography (upper panels in A and B) for 20 d ([³H]myristate) or 2 mo ([³H]palmitate). The lower panels in A and B depict Western blots (rabbit anti-GFP) of Src- or Fyn-GFP from the immunoprecipitate of each sample. Sample processing was as described under *Materials and Methods*. (A, B) Fluorography (top panels) and Western blotting (bottom panels) results of typical experiments. (C, D) Quantification (mean \pm SEM, $n = 3$) of the incorporation of [³H]myristate (C) and [³H]palmitate (D) into the GFP-tagged proteins. Bands for myristate or palmitate incorporation and of the GFP-tagged proteins were quantified by densitometry and normalized for protein level by the respective Western blot of the same immunoprecipitate. For [³H]myristate, the normalized value obtained for Src-GFP was taken as 100%; for [³H]palmitate, the analogous value obtained for Fyn-GFP was set as 100%. Asterisks indicate significant differences between the pairs indicated by the brackets (*, $p < 10^{-2}$; Student's *t* test).

sites of Fyn (the Fyn-C3S/C6S mutant) shifted the distribution of the mutated protein to non-DRM fractions, in accord with regulation of the domain distribution of the SFK mutants by the palmitoylation of their N-terminal region.

To complement the above experiments, we investigated the interactions of Fyn (WT and constitutively active) with Cav-1 in the membrane of live cells. To this end, we coexpressed a Fyn-GFP protein together with Cav-1-mRFP or Cav-1-Y14F-mRFP (a Cav-1 mutant lacking the Tyr-14 Src phosphorylation site). Coexpressing cells were identified by green and red fluorescence, respectively and subjected to FRAP beam-size analysis to measure the effect of Cav-1 or Cav-1-Y14F on the membrane interactions of the Fyn-GFP protein. As shown in Figure 7, A and B, Cav-1-WT slowed the FRAP rate of Fyn-WT-GFP and elevated its $\tau(40x)/\tau(63x)$ ratio to a level indistinguishable from the beam-size ratio, suggesting enhanced membrane interactions. Interestingly, this effect did not require SFK-mediated phosphorylation of Cav-1 on Tyr-14, since the phosphorylation-defective Cav-1-Y14F induced even a somewhat stronger effect in the same direction. On the other hand, neither the FRAP rate nor the τ ratio of the constitutively active Fyn-Y531F-GFP mutant was affected by either Cav-1-WT or Cav-1-Y14F (Figure 7, C and D), in line with the notion that its stronger membrane interactions are due to transient binding of the open conformation to a

large population of pTyr membrane protein targets, as was shown for Src (Shvartsman *et al.*, 2007; see Figure 4). Of note, The effects of Cav-1 on the membrane interactions of Fyn-WT-GFP and Fyn-Y531F-GFP, which are the first such demonstration, are a mirror image of our earlier findings on the effects of Cav-1 on Src-GFP membrane interactions (Gottlieb-Abraham *et al.*, 2013), where only constitutively active Src-Y527F-GFP (but not Src-WT-GFP) was slowed by coexpression with Cav-1, an effect that the Cav-1-Y14F mutant was incapable of. We conclude that unlike Src, whose activated form phosphorylates Cav-1-WT and then colocalizes with the phosphorylated Cav-1 (pCav-1, phosphorylated at Tyr-14) in focal adhesions, Fyn binds to Cav-1 already in its inactive state and does not follow pCav-1 out of the caveolae/raft domains. Thus the binding of Fyn-WT to Cav-1 contributes to the preferential association of Fyn with rafts/caveolae. This conclusion is in accord with the report that another raft-resident protein, Csk-binding protein (Cbp), suppresses SFK-mediated cell transformation with strong correlation to the ability of the SFK to undergo palmitoylation and distribute into rafts/caveolae (Oneyama *et al.*, 2008, 2009).

DISCUSSION

Association with the membrane is critical for SFK signaling, and cytoplasmic forms of Src (e.g., due to lack of myristoylation) have defective signaling and fail to transform cells (Kamps *et al.*, 1985, 1986; Linder and Burr, 1988; Patwardhan and Resh, 2010). The membrane interactions of SFKs are mediated by the fatty-acylated N-terminal membrane anchor, which differs between SFKs and regulates their distribution to distinct cellular regions/domains (Shenoy-Scaria *et al.*, 1994; Sigal *et al.*, 1994; Melkonian *et al.*, 1999; Resh, 1999, 2006). The differences between SFKs in the palmitoylation of the N-terminal anchor largely dictate both their membrane interactions and their targeting to lipid rafts/caveolae, and it was proposed that differential sequestration in such domains may regulate the transforming potential of SFKs (Oneyama *et al.*, 2008, 2009; Cai *et al.*, 2011; Gottlieb-Abraham *et al.*, 2013). However, the relations between the factors that contribute to the membrane anchoring and domain-targeting functions of the N-terminal region remained enigmatic. Here, using GFP-tagged Src and Fyn (WT and mutants), we demonstrate for the first time that palmitoylation of the N-terminal anchor enhances and stabilizes SFK membrane association relative to a polybasic cluster. First, our findings show that effective myristoylation and consequent palmitoylation depend on the initial N-terminal sequence (Gly-2 to Lys-7). Second, they demonstrate that the charged Lys-5 (the first positively charged residue in the Src polybasic cluster) strongly reduces myristoylation (and therefore palmitoylation) when Ser-3/6 are replaced by Cys, suggesting that Lys-5 can be tolerated when Ser-6 (preferred by NMT) is retained, but not when it is replaced by Cys. While palmitoylation is known to preferentially target SFKs to DRMs, we show here that unlike Src, the

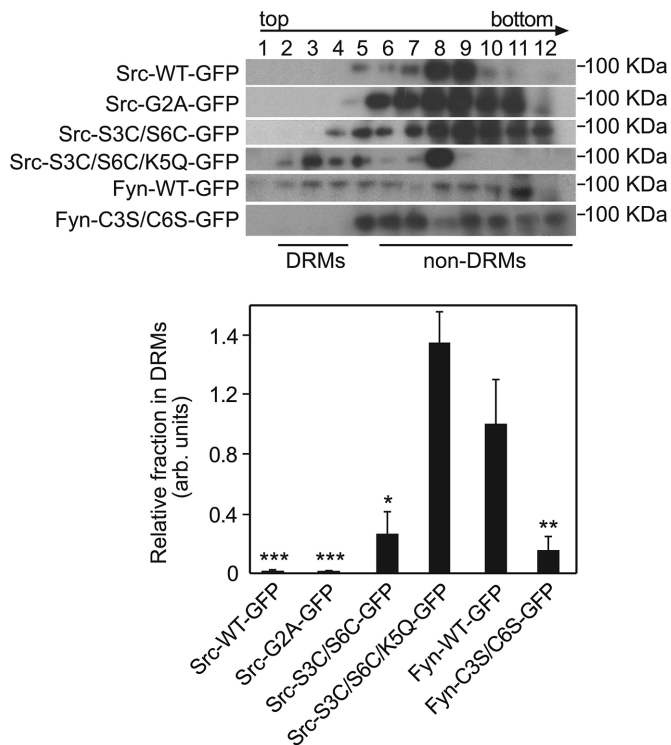


FIGURE 6: Distribution of Src and Fyn palmitoylation mutants to DRMs. Cells expressing the indicated Src-GFP or Fyn-GFP proteins were lysed and fractionated using a three-step sucrose gradient as described, resulting in fractions 2–4 (Oneyama *et al.*, 2009; see *Materials and Methods*). Fractions of 1 ml were collected from top (fraction 1) to bottom (fraction 12). After precipitation of the proteins by TCA, samples were subjected to Western blotting for GFP (see *Materials and Methods*), and the SFK-GFP bands were quantified by densitometry. (A) Typical results of a fractionation experiment. (B) Quantification (mean \pm SEM, $n = 3$) of the fractions in DRMs. Results were normalized relative to the DRM fraction of Fyn-WT-GFP, which was assigned the value of 1. Asterisks designate significant differences between a given mutant and Fyn-WT-GFP (*, $p < 0.05$; **, $p < 10^{-2}$; ***, $p < 10^{-8}$; Student's *t* test).

dual-palmitoylated Fyn binds to Cav-1 already in its unactivated (WT) form, and this interaction does not require phosphorylation of Cav-1 at Tyr-14. Our findings support a mechanism whereby activation of nonraft signaling pathways is restricted by sequestration of palmitoylated SFKs in rafts/caveolae, limiting their transforming potential.

Membrane targeting of SFKs was shown to require myristoylation at Gly-2 by NMT and a second signal, provided by either a polybasic cluster or palmitoylation site(s) in the N-terminal anchor region. Here we compared the membrane interactions conferred by the two types of second signals by direct biophysical studies (FRAP beam-size analysis) in live cells. As shown in Figures 1–3, the membrane interactions conferred by palmitoylation as the second signal (Fyn and the Src-S3C/S6C/K5Q mutant) are stronger than when the second signal is a polybasic cluster (Src-WT). The novel demonstration of the enhanced membrane interactions of Fyn and Src-S3C/S6C/K5Q is evident from their higher $\tau(40x)/\tau(63x)$ ratio, which is significantly closer to the beam-size ratio of 2.28, suggesting recovery by pure lateral diffusion, attesting to a lower contribution of exchange relative to lateral diffusion (more stable membrane interactions; discussed in Henis *et al.*, 2006; Shvartsman *et al.*, 2007; Eisenberg *et al.*, 2011). The higher τ ratios of the palmitoylated proteins are

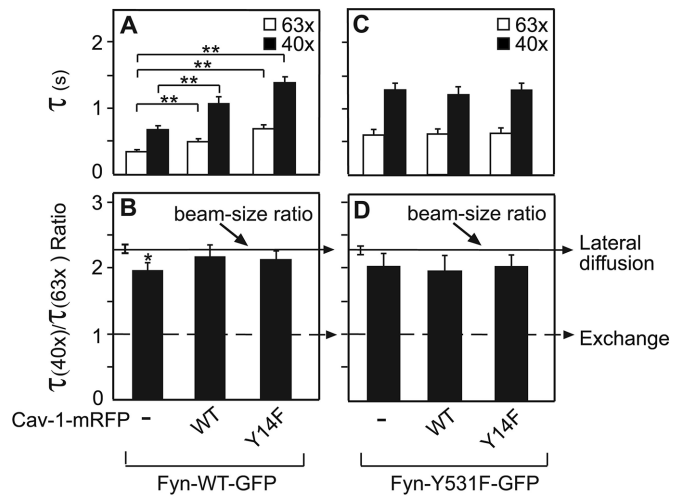


FIGURE 7: Cav-1-WT and Cav-1-Y14F enhance the membrane interactions of Fyn-WT but not Fyn-Y531F. Cells were cotransfected with a vector encoding Fyn-WT-GFP or Fyn-Y531F-GFP, together with an expression vector for Cav-1-WT-mRFP, Cav-1-Y531F-mRFP, or empty vector (control). After 24 h, FRAP beam-size analysis was conducted on Fyn-WT-GFP (A, B) or Fyn-Y531F-GFP (C, D) as in Figure 1. Bars, means \pm SEM of 30–60 measurements. (A, C) τ values. Significant effects of Cav-1 or Cav-1-Y14F were observed only on Fyn-WT-GFP. Asterisks indicate significant differences between the $\tau(63x)$ or $\tau(40x)$ values of the pairs indicated by the brackets, comparing τ values measured with the same beam size (**, $p < 10^{-5}$; Student's *t* test). (B, D) $\tau(40x)/\tau(63x)$ ratios. Only the τ ratio of Fyn-WT without coexpression of Cav-1 was below the 2.28 value expected for lateral diffusion (*, $p < 10^{-2}$). All other τ ratios were not significantly different from the 2.28 beam-size ratio, indicating stable interactions with the plasma membrane.

accompanied by slower FRAP rates, in line with the lower contribution of exchange (Figures 1 and 3).

An interesting point demonstrated in these studies is the interdependence of the distinct N-terminal membrane-targeting signals (myristoylation, palmitoylation, and a positively charged cluster). Src has Ser residues at position 3 and 6, whose mutation to cysteines (Src-S3C/S6C) was assumed to result in a palmitoylation-capable Src mutant (Sandilands *et al.*, 2007; Cai *et al.*, 2011). However, our biophysical studies clearly show that this mutant is mainly cytoplasmic, exhibiting very fast FRAP kinetics that are only twofold slower than those of the myristoylation-defective, cytoplasmic Src-G2A (Figures 1 and 3). In accord with the notion that Src-S3C/S6C has defective palmitoylation, its FRAP behavior is unaffected by the palmitoylation inhibitor 2BP (Figure 2). The biochemical data on myristoylation and palmitoylation of these mutants (Figure 5) directly validate the defective palmitoylation of Src-S3C/S6C, revealing that it occurs due to a strong reduction of its myristoylation. Importantly, the defects in myristoylation along with the ensuing palmitoylation were released concomitantly by replacing the positively charged Lys-5 with Gln, which appears at this position in Fyn (Src-S3C/S6C/K5Q; Figure 5), accompanied by regaining the membrane association, which became very close to that of Fyn (Figure 3). These findings are in agreement with the N-terminal sequence motifs recognized by eukaryotic NMTs, which attach the myristoyl to Gly-2 (counting Met-1 as the first residue): while the small, polar Ser is preferred for NMT recognition at positions 6 (and to a lesser degree at 3; Resh, 1999; Maurer-Stroh *et al.*, 2002), large hydrophobic residues are preferred at position 5 (Maurer-Stroh *et al.*, 2002). In Src, position 5 is occupied by Lys, which is not only nonhydrophobic, but

charged. Apparently, this misfit can be tolerated due to the Ser residues at the preferred 6 and 3 positions. Ser-6 appears to be of the highest importance, since S6C mutation in v-Src reduced its myristoylation, while S3C mutation had no effect (Alland *et al.*, 1994). When this preference is compromised by replacing these serines with cysteines (imitating Fyn, in the Src-S3C/S6C mutant), the presence of the charged Lys-5 becomes highly disruptive, and its replacement by the neutral Gln5 as in Fyn is necessary for restoring effective myristoylation and palmitoylation (the Src-S3C/S6C/K5Q mutant). Of note, the dependence of Src myristoylation on the above residues reflects the preference reported for NMT enzymes and is not absolute. This is exemplified by the low but detectable level of myristoylation observed for Src-S3C/S6C (Figure 5). Apparently, once a molecule of Src-S3C/S6C is myristoylated, it can also undergo palmitoylation; therefore the level of palmitoylation of this mutant is also detectable but significantly lower than that of Fyn-WT (Figure 5).

The above findings were obtained on cells expressing unactivated Src/Fyn or their mutants. In view of our former demonstration that the membrane interactions of activated Src are significantly stronger than those of the unactivated folded conformation, due to its ability to phosphorylate membrane protein targets and then bind to the pTyr sites via its SH2 domain (Shvartsman *et al.*, 2007), it was of interest to explore the membrane interactions of distinct Src and Fyn proteins in their constitutively active, open conformation. Figure 4 shows that Fyn-Y531F membrane interactions were essentially identical to those obtained for constitutively active Src-Y527F, exhibiting a high τ ratio similar to the beam size ratio (i.e., negligible contribution of exchange, in line with stable membrane interactions), and slower FRAP rates (higher τ values) suggesting that the mobility retardation is due to transient binding to slower-diffusing transmembrane proteins (Shvartsman *et al.*, 2007; Gottlieb-Abraham *et al.*, 2013). These results are in accord with our findings on the membrane interactions of activated Src (Shvartsman *et al.*, 2007; Gottlieb-Abraham *et al.*, 2013) and suggest that activated Fyn is capable of interacting with membrane protein target sites in a similar manner. On the other hand, a constitutively active mutant of the myristoylation/palmitoylation-defective Src-S3C/S6C mutant (Src-S3C/S6C/Y527F) retained the mainly cytoplasmic phenotype, exhibiting very fast cytoplasmic-like diffusion. The failure of this constitutively active mutant, which has a fatty acylation-defective N-terminal anchor, to bind to membrane protein targets via its SH2 domain provides the first demonstration that the N-terminal anchor has a necessary role in the initial targeting of activated Src to the membrane. Only when the initial targeting takes place can the protein effectively phosphorylate target proteins and bind to their pTyr sites. This observation is in agreement with the inactive nature of cytoplasmic Src (Newsome *et al.*, 2006; Patwardhan and Resh, 2010).

In view of the reports that dual palmitoylation of SFKs targets them to lipid rafts and caveolae (Shenoy-Scaria *et al.*, 1994; Robbins *et al.*, 1995; Resh, 1999; Suzuki *et al.*, 2007; Oneyama *et al.*, 2009), we investigated the association of the Src and Fyn palmitoylation mutants with DRMs and Cav-1, which is a major constituent of caveolae. The results of the studies on partitioning into DRMs (Figure 6) are in accord with the notion that palmitoylation directs SFKs to raft domains. This is demonstrated by the significantly higher fraction of palmitoylated Fyn or Src proteins in DRMs (Fyn-WT and Src-S3C/S6C/K5Q) relative to their nonpalmitoylated counterparts (Src-WT and Fyn-C3S/C6S). Analogously, Fyn-WT membrane interactions were enhanced upon coexpression with Cav-1 (Figure 7), while our previous studies demonstrated that Cav-1 expression

fails to enhance the membrane interactions of Src-WT (Gottlieb-Abraham *et al.*, 2013). It is important to note that Cav-1-Y14F, which lacks the Tyr-14 Src phosphorylation target site, enhanced the membrane interactions of Fyn-WT and retarded its FRAP kinetics even more than Cav-1-WT (Figure 7). This demonstrates that phosphorylation of Cav-1 on Tyr-14 is dispensable for its interactions with Fyn-WT, in line with the inability of Cav-1-WT or Cav-1-Y14F to significantly enhance the membrane interactions of activated Fyn (Fyn-Y531F; Figure 7, C and D). The insensitivity of Fyn-Y531F membrane interactions to overexpression of Cav-1 contrasts with our findings on activated Src-Y527F, which phosphorylated Cav-1 at Tyr-14, bound pCav-1 via its SH2 domain, and followed it to focal adhesions (Gottlieb-Abraham *et al.*, 2013). This major difference between Fyn and Src in the interactions with DRMs and Cav-1, where Fyn-WT interacts with Cav-1 and with DRMs in its unactivated form, while Src has a much lower fraction in DRMs and interacts with pCav-1 mainly in its active conformation, may explain not only why Cav-1 phosphorylation is not required for its interaction with Fyn-WT, but also the stronger effect of Cav-1-Y14F on Fyn-WT membrane interactions. It is tempting to speculate that Cav-1-Y14F may be more prominent in caveolae than Cav-1-WT, since only the latter can equilibrate between caveolae and other cellular structures (such as focal adhesions), depending on its phosphorylation on Tyr-14.

The results described above are in agreement with the reports that the raft-resident protein Cbp helps to recruit SFKs to rafts/caveolae and that increased confinement of specific SFKs in such domains correlates with their palmitoylation and suppresses SFK-mediated cell transformation (Oneyama *et al.*, 2008, 2009; Cai *et al.*, 2011). We propose that targeting of activated SFKs to rafts versus nonraft sites (such as focal adhesions) can serve as a competitive mechanism that regulates cell transformation by SFKs. Containment of palmitoylated SFKs (e.g., Fyn) in raft domains is at the expense of their distribution to nonraft sites, where their protumorigenic activity is expressed, in line with their lower transformation potential (Oneyama *et al.*, 2008, 2009; Cai *et al.*, 2011). Thus specific SFKs (such as Fyn) can be targeted to rafts/caveolae by their palmitoylation and affinity to raft proteins such as Cbp and/or Cav-1, while SFKs that lack palmitoylation (e.g., Src) display a weaker affinity to rafts and are targeted to nonraft pTyr-protein targets (e.g., the preferential binding of activated Src SH2 domain to pCav-1 in focal adhesions), enhancing their metastatic potential.

MATERIALS AND METHODS

Reagents

Rabbit antibodies to GFP (FL) (sc-8334) were from Santa Cruz Biotechnology (Santa Cruz, CA). The anti-GFP (FL) antibody served for blotting, while for immunoprecipitation a sheep anti-GFP antibody was used; this antibody, described earlier (Laude and Prior, 2008), was a generous gift from I. A. Prior, University of Liverpool, UK. Mouse anti- β -actin (antibody 4) was from MP Biomedicals (Santa Ana, CA), and peroxidase-conjugated goat anti-rabbit immunoglobulin G (IgG; catalogue number 111-035-003) from Jackson ImmunoResearch Laboratories (West Grove, PA). Immobilized Protein A and GammaBind-Sepharose were from GE Healthcare (Little Chalfont, UK). [9,10- 3 H]Palmitic acid and [9,10- 3 H]myristic acid, 30–60 Ci (1.11–2.22 TBq)/mmol each, were from Hartmann Analytic (Braunschweig, Germany). Protease inhibitor cocktail (P8340), Na₃VO₄, and the palmitoylation inhibitor 2-bromopalmitate (2BP) were from Sigma-Aldrich (St. Louis, MO). Restriction enzymes and T4 DNA ligase were from New England Biolabs (Ipswich, MA). Hank's balanced salts solution (HBSS), DMEM, fetal calf serum (FCS), penicillin-streptomycin solution and glutamine were purchased from

Biological Industries (Beit Haemek, Israel). All other reagents were from Sigma-Aldrich.

Plasmids

Biologically active pEGFP-N1 expression vectors for chicken c-Src (Src-WT-GFP, constitutively active Src-Y527F-GFP and a Ser-to-Cys N-terminal replacement mutant, Src-S3C/S6C-GFP), as well as for human Fyn (Fyn-WT-GFP, the constitutively active Fyn-Y531F-GFP derived from it, and a Cys-to-Ser replacement N-terminal Fyn mutant, Fyn-C3S/C6S-GFP) (described in Sandilands *et al.*, 2004, 2007) were donated by M. C. Frame (University of Edinburgh, UK). Canine Cav-1-mRFP in pcDNA3.1 (+) (Sharma *et al.*, 2004) was a gift from R. E. Pagano (Mayo Clinic, Rochester, MN) and was mutated to generate an expression vector for Cav-1-Y14F-mRFP (Gottlieb-Abraham *et al.*, 2013).

Additional Src and Fyn mutants were created by site-directed mutagenesis using the QuickChange mutagenesis kit (Stratagene, La Jolla, CA). The nonmyristoylated Src mutant Src-G2A-GFP (Gly-2 replaced by Ala) was created using Src-WT-GFP as template, with the forward primer 5'-AGGAGGTACGACCATGGCGAGCAGCAAG-AGCAAGC-3' and the reverse primer 5'-GCTTGCTCTTGCTGCTC-GCCATGGTCGTAC-CTCCT-3'. Src-S3C/S6C-GFP served as template to generate the triple Src mutants Src-S3C/S6C/K5Q-GFP and Src-S3C/S6C/Y527F-GFP. The primers used were 5'-ATGGGGTG-TAGCCAGTGTAAGCCCAAGG-3' (forward) and 5'-CCTTGGGCT-TACTGCTACACCCCAT-3' (reverse) for the K5Q mutation (underlined); or 5'-CGACAGAGCCCCAGTTCAGCCTGGAGAGAAC-3' (forward) and 5'-GTTCTCTCCAGGCTGGAAGTGGGGCTCTGTCCG-3' (reverse) for the Y527F mutation (underlined). Src-S3C/S6C/K5Q-GFP served as template to generate the constitutively active mutant Src-S3C/S6C/K5Q/Y527F-GFP, using the primers 5'-CGACAG-AGCCCCAGTTCAGCCTGGAGAGAAC-3' (forward) and 5'-GTTCTCTCCAGGCTG-GAAGTGGGGCTCTGTCCG-3' (reverse). All mutants were verified by sequencing.

Cell culture and transfections

COS7 cells (CRL 1651) were from the American Type Culture Collection (Manassas, VA). They were grown in DMEM containing 10% FCS as described earlier (Shvartsman *et al.*, 2003). For FRAP studies, the cells were grown on glass coverslips placed in six-well plates and transfected using TransIT-LT1 (Mirus Bio LLC, Madison, WI) with a vector encoding a Src-GFP (0.15 μ g DNA) or Fyn-GFP (0.30 μ g DNA) derivative. In some experiments, the cells were cotransfected with one of the above vectors together with Cav-1-mRFP or Cav-1-Y14F-mRFP (0.30 μ g) or empty pcDNA3.1 vector (control). The total DNA level was completed to 0.6 μ g in all cases by empty pcDNA3.1 vector. For biochemical studies, cells grown in 60-mm (metabolic labeling) or 100mm (subcellular fractionation experiments) dishes were transfected similarly, except that the DNA amounts were increased by the factor of the surface area of the dish (x2.9 for 6-mm dish and x8.2 for 100-mm dish).

FRAP beam-size analysis

At 24 h posttransfection, COS7 cells expressing Src-GFP or Fyn-GFP proteins (alone or together with a Cav-1-mRFP construct) were taken for FRAP studies, conducted in HBSS supplemented with 20 mM HEPES, pH 7.2 (HBSS/HEPES). In some experiments, cells were first subjected to treatment with the palmitoylation inhibitor 2BP (50 μ M, 18 h) initiated at 6 h posttransfection (Eisenberg *et al.*, 2013). To minimize internalization, FRAP measurements were at 22°C, replacing samples within 15 min. An argon ion laser beam (Innova 70C; Coherent, Santa Clara, CA) was focused through a fluorescence microscope

(AxioImager.D1; Carl Zeiss MicroImaging, Jena, Germany) to a spot with a Gaussian radius (ω) of $0.77 \pm 0.03 \mu\text{m}$ (plan apochromat 63x/1.4 NA oil-immersion objective) or $1.17 \pm 0.05 \mu\text{m}$ (C apochromat 40x/1.2 NA water-immersion objective), and experiments were conducted with each objective (beam-size analysis; Henis *et al.*, 2006). The ratio between the bleached areas was 2.28 ± 0.17 ($n = 59$). After a brief measurement at the monitoring laser intensity (488 nm, 1 μ W), a 5-mW pulse (5–10 ms) bleached 60–75% of the fluorescence in the illuminated spot, and fluorescence recovery was followed by the monitoring beam. The characteristic fluorescence recovery time (τ) and mobile fraction (R_f) were extracted from the FRAP curves by nonlinear regression analysis, fitting to a lateral diffusion process (Henis *et al.*, 2006). The R_f values for all Src-GFP or Fyn-GFP proteins were above 0.95 in all cases.

Statistical analysis of FRAP data

The significance of differences between τ values measured by FRAP with the same laser beam size was evaluated by Student's *t* test. To compare measurements of the ratio between the values of the characteristic recovery times (τ) obtained with the 40x and 63x objectives or the areas illuminated by the laser beam using these objectives ($\tau(40x)/\tau(63x)$ and $\omega^2(40x)/\omega^2(63x)$, respectively; see *Results*), we used bootstrap analysis, which is preferable for comparison between ratios (Efron and Tibshirani, 1993). The bootstrap analysis was carried out exactly as described by us earlier (Gutman *et al.*, 2010), using 1000 bootstrap samples.

Immunoblotting

COS7 cells grown in 60- or 100-mm dishes were transfected with Src-GFP or Fyn-GFP expression vectors. They were subjected to lysis in lysis buffer 1 (50 mM HEPES, pH 7.5, 100 mM NaCl, 5 mM MgCl₂, 1 mM egtazic acid (EGTA), 1% NP-40, 0.1% lauryl maltoside, protease inhibitor cocktail, and 0.1 mM Na₃VO₄) for metabolic labeling experiments, or in lysis buffer 2 (50 mM Tris, pH 7.4, 150 mM NaCl, 0.25% Triton X-100, 1 mM EDTA, 20 mM NaF, protease inhibitor cocktail, and 1 mM Na₃VO₄) for subcellular fractionation experiments, following the protocol used earlier for measuring SFKs localization in DRMs (Oneyama *et al.*, 2009). After low-speed centrifugation to remove nuclei and cell debris, the lysates were subjected to SDS-PAGE (7.5% acrylamide) and immunoblotting as described (Kfir *et al.*, 2005). The blots were probed (12 h, 4°C) by primary antibodies (rabbit anti-GFP at 1:5000), followed by peroxidase-coupled goat anti-rabbit IgG (1:10,000 for 1 h at 22°C). Bands were visualized by ECL (Western Bright; Advansta, Menlo Park, CA) and quantified by densitometry (EZQuant-Gel 2.2; EZQuant Ltd., Tel Aviv, Israel).

Metabolic labeling with [³H]palmitic or [³H]myristic acid

COS7 cells were grown in 60-mm-diameter dishes and transfected with plasmid DNA. [9,10-³H]palmitic acid or [9,10-³H]myristic acid (30–60 Ci/mmol, in ethanol) were concentrated by evaporation under a constant stream of nitrogen and resuspended in 200 μ l ethanol. Cells were labeled at 24 h posttransfection for 12 h with 400 μ Ci of [³H]-labeled palmitate or myristate in 2 ml/dish of DMEM supplemented with 10% FCS previously dialyzed against sterile 0.9% NaCl. The dishes were placed on ice, washed twice with cold phosphate-buffered saline, and lysed in 0.5 ml ice-cold lysis buffer 1. After removal of cell debris by centrifugation, the lysates were subjected to immunoprecipitation with 2 μ g sheep anti-GFP per sample as described (Shvartsman *et al.*, 2007), using a 1:1 mix of protein A and GammaBind-sepharose. To preserve protein acylation, samples were not boiled prior to electrophoresis, but instead were incubated

in SDS-loading solution lacking reducing agents for at least 1 h at room temperature. Samples were then resolved by SDS-PAGE under nonreducing conditions at low amperage overnight in the cold. A fraction of each sample (10%) was processed for Src-GFP or Fyn-GFP by Western blotting (see *Immunoblotting*), while the remainder (90%) was fixed after blotting (isopropanol:water:acetic acid 25:65:10, 30 min) and processed by fluorography to measure the levels of incorporation of [³H]palmitate and [³H]myristate (Song *et al.*, 2013). For the latter, gels were soaked in Amplify (GE Healthcare), dried and exposed to a film for 20 d ([³H]myristate) or 2 mo ([³H]palmitate).

Subcellular fractionation

For fractionation of raft (DRM) and nonraft (non-DRM) membrane fractions, we used the discontinuous sucrose gradient flotation procedure described earlier for SFKs (Oneyama *et al.*, 2008, 2009). This procedure results in DRMs (identified by cholera toxin B-subunit labeled GM1 ganglioside) appearing in fractions 2–4 (Oneyama *et al.*, 2008, 2009). COS7 cells expressing a Src-GFP or Fyn-GFP protein were lysed with lysis buffer 2, cleared by low-speed centrifugation, and separated on a three-step sucrose gradient (5, 35, and 40% sucrose) by ultracentrifugation (6 h, 4°C) at 40,000 × g in a SW40 rotor (Beckman Coulter, Brea, CA). Twelve 1 ml fractions were collected from the top of the gradient. Proteins were precipitated with 20% trichloroacetic acid after addition of 2 μg BSA as carrier, resuspended in 50 μl of 2x sample buffer, and mixed with 50 μl of 1 M Tris (pH 8). From this, 50 μl was taken for analysis by SDS-PAGE followed by immunoblotting for GFP.

ACKNOWLEDGMENTS

This work was supported in part by a grant from the Israel Cancer Association through the estate of the late Alexander Smidoda (to Y. I. H.) and by grant RTG1715 from the German Research Council (DFG) (to I.R.). Y. I. H. is an incumbent of the Zalman Weinberg Chair in Cell Biology. We thank M. C. Frame and R. E. Pagano for their generous donation of plasmids and I. A. Prior for providing the sheep anti-GFP antibody.

REFERENCES

Abram CL, Courtneidge SA (2000). Src family tyrosine kinases and growth factor signaling. *Exp Cell Res* 254, 1–13.

Ahearn IM, Tsai FD, Court H, Zhou M, Jennings BC, Ahmed M, Fehrenbacher N, Linder ME, Philips MR (2011). FKBP12 binds to acylated H-ras and promotes depalmitoylation. *Mol Cell* 41, 173–185.

Alland L, Peseckis SM, Atherton RE, Berthiaume L, Resh MD (1994). Dual myristylation and palmitoylation of Src family member p59^{fyn} affects subcellular localization. *J Biol Chem* 269, 16701–16705.

Boggan TJ, Eck MJ (2004). Structure and regulation of Src family kinases. *Oncogene* 23, 7918–7927.

Brown MT, Cooper JA (1996). Regulation, substrates and functions of src. *Biochim Biophys Acta* 1287, 121–149.

Cai H, Smith DA, Memarzadeh S, Lowell CA, Cooper JA, Witte ON (2011). Differential transformation capacity of Src family kinases during the initiation of prostate cancer. *Proc Natl Acad Sci USA* 108, 6579–6584.

Efron B, Tibshirani R (1993). Estimates of bias. In: *An Introduction to Bootstrap*, ed. DR Cox, DV Hinkley, N Reid, DB Rubin, and BW Silverman, London: Chapman & Hall, 124–130.

Eisenberg S, Beckett AJ, Prior IA, Dekker FJ, Hedberg C, Waldmann H, Ehrlich M, Henis YI (2011). Raft protein clustering alters N-Ras membrane interactions and activation pattern. *Mol Cell Biol* 31, 3938–3952.

Eisenberg S, Laude AJ, Beckett AJ, Mageean CJ, Aran V, Hernandez-Valladares M, Henis YI, Prior IA (2013). The role of palmitoylation in regulating Ras localization and function. *Biochem Soc Trans* 41, 79–83.

Farazi TA, Waksman G, Gordon JI (2001). The biology and enzymology of protein N-myristoylation. *J Biol Chem* 276, 39501–39504.

Frame MC (2004). Newest findings on the oldest oncogene; how activated src does it. *J Cell Sci* 117, 989–998.

Gottlieb-Abraham E, Shvartsman DE, Donaldson JC, Ehrlich M, Gutman O, Martin GS, Henis YI (2013). Src-mediated Caveolin-1 phosphorylation affects the targeting of active Src to specific membrane sites. *Mol Biol Cell* 24, 3881–3895.

Gutman O, Walliser C, Piechulek T, Gierschik P, Henis YI (2010). Differential regulation of phospholipase C-β₂ activity and membrane interaction by Gα_q, Gβ₁g₂, and Rac2. *J Biol Chem* 285, 3095–3015.

Hancock JF (2003). Ras proteins: different signals from different locations. *Nat Rev Mol Cell Biol* 4, 373–384.

Hancock JF (2006). Lipid rafts: contentious only from simplistic standpoints. *Nat Rev Mol Cell Biol* 7, 456–462.

Henis YI, Hancock JF, Prior IA (2009). Ras acylation, compartmentalization and signaling nanoclusters. *Mol Membr Biol* 26, 80–92.

Henis YI, Rotblat B, Kloog Y (2006). FRAP beam-size analysis to measure palmitoylation-dependent membrane association dynamics and microdomain partitioning of Ras proteins. *Methods* 40, 183–190.

Ingley E (2008). Src family kinases: regulation of their activities, levels and identification of new pathways. *Biochim Biophys Acta* 1784, 56–65.

Irby RB, Yeatman TJ (2000). Role of Src expression and activation in human cancer. *Oncogene* 19, 5636–5642.

Jacobson K, Mouritsen OG, Anderson RG (2007). Lipid rafts: at a crossroad between cell biology and physics. *Nat Cell Biol* 9, 7–14.

Kamps MP, Buss JE, Sefton BM (1985). Mutation of NH₂-terminal glycine of p60^{src} prevents both myristoylation and morphological transformation. *Proc Natl Acad Sci USA* 82, 4625–4628.

Kamps MP, Buss JE, Sefton BM (1986). Rous sarcoma virus transforming protein lacking myristic acid phosphorylates known polypeptide substrates without inducing transformation. *Cell* 45, 105–112.

Kfir S, Ehrlich M, Goldshmid A, Liu X, Kloog Y, Henis YI (2005). Pathway- and expression level-dependent effects of oncogenic N-Ras: p27^{KIP1} mislocalization by the Ral-GEF pathway and Erk-mediated interference with Smad signaling. *Mol Cell Biol* 25, 8239–8250.

Koegl M, Zlatkine P, Ley SC, Courtneidge SA, Magee AI (1994). Palmitoylation of multiple Src-family kinases at a homologous N-terminal motif. *Biochem J* 303, Pt 3749–753.

Laude AJ, Prior IA (2008). Palmitoylation and localisation of RAS isoforms are modulated by the hypervariable linker domain. *J Cell Sci* 121, 421–427.

Linder ME, Burr JG (1988). Nonmyristoylated p60^{v-src} fails to phosphorylate proteins of 115–120 kDa in chicken embryo fibroblasts. *Proc Natl Acad Sci USA* 85, 2608–2612.

Martin GS (2001). The hunting of the Src. *Nat Rev Mol Cell Biol* 2, 467–475.

Maurer-Stroh S, Eisenhaber B, Eisenhaber F (2002). N-terminal N-myristoylation of proteins: refinement of the sequence motif and its taxon-specific differences. *J Mol Biol* 317, 523–540.

McLaughlin S, Aderem A (1995). The myristoyl-electrostatic switch: a modulator of reversible protein-membrane interactions. *Trends Biochem Sci* 20, 272–276.

Melkonian KA, Ostermeyer AG, Chen JZ, Roth MG, Brown DA (1999). Role of lipid modifications in targeting proteins to detergent-resistant membrane rafts. Many raft proteins are acylated, while few are prenylated. *J Biol Chem* 274, 3910–3917.

Newsome TP, Weisswange I, Frischknecht F, Way M (2006). Abl collaborates with Src family kinases to stimulate actin-based motility of vaccinia virus. *Cell Microbiol* 8, 233–241.

Oneyama C, Hikita T, Enya K, Dobenecker MW, Saito K, Noda S, Tarakhovskiy A, Okada M (2008). The lipid raft-anchored adaptor protein Cbp controls the oncogenic potential of c-Src. *Mol Cell* 30, 426–436.

Oneyama C, Iino T, Saito K, Suzuki K, Ogawa A, Okada M (2009). Transforming potential of Src family kinases is limited by the cholesterol-enriched membrane microdomain. *Mol Cell Biol* 29, 6462–6472.

Parton RG, del Pozo MA (2013). Caveolae as plasma membrane sensors, protectors and organizers. *Nat Rev Mol Cell Biol* 14, 98–112.

Patwardhan P, Resh MD (2010). Myristoylation and membrane binding regulate c-Src stability and kinase activity. *Mol Cell Biol* 30, 4094–4107.

Resh MD (1994). Myristoylation and palmitoylation of Src family members: the fats of the matter. *Cell* 76, 411–413.

Resh MD (1999). Fatty acylation of proteins: new insights into membrane targeting of myristoylated and palmitoylated proteins. *Biochim Biophys Acta* 1451, 1–16.

Resh MD (2006). Trafficking and signaling by fatty-acylated and prenylated proteins. *Nat Chem Biol* 2, 584–590.

Robbins SM, Quintrell NA, Bishop JM (1995). Myristoylation and differential palmitoylation of the HCK protein-tyrosine kinases govern their attachment to membranes and association with caveolae. *Mol Cell Biol* 15, 3507–3515.

- Sandilands E, Brunton VG, Frame MC (2007). The membrane targeting and spatial activation of Src, Yes and Fyn is influenced by palmitoylation and distinct RhoB/RhoD endosome requirements. *J Cell Sci* 120, 2555–2564.
- Sandilands E, Cans C, Fincham VJ, Brunton VG, Mellor H, Prendergast GC, Norman JC, Superti-Furga G, Frame MC (2004). RhoB and actin polymerization coordinate Src activation with endosome-mediated delivery to the membrane. *Dev Cell* 7, 855–869.
- Sharma DK, Brown JC, Choudhury A, Peterson TE, Holicky E, Marks DL, Simari R, Parton RG, Pagano RE (2004). Selective stimulation of caveolar endocytosis by glycosphingolipids and cholesterol. *Mol Biol Cell* 15, 3114–3122.
- Shenoy-Scaria AM, Dietzen DJ, Kwong J, Link DC, Lublin DM (1994). Cysteine3 of Src family protein tyrosine kinase determines palmitoylation and localization in caveolae. *J Cell Biol* 126, 353–363.
- Shvartsman DE, Donaldson JC, Diaz B, Gutman O, Martin GS, Henis YI (2007). Src kinase activity and SH2 domain regulate the dynamics of Src association with lipid and protein targets. *J Cell Biol* 178, 675–686.
- Shvartsman DE, Kotler M, Tall RD, Roth MG, Henis YI (2003). Differently-anchored influenza hemagglutinin mutants display distinct interaction dynamics with mutual rafts. *J Cell Biol* 163, 879–888.
- Sicheri F, Moarefi I, Kuriyan J (1997). Crystal structure of the Src family tyrosine kinase Hck. *Nature* 385, 602–609.
- Sigal CT, Zhou W, Buser CA, McLaughlin S, Resh MD (1994). Amino-terminal basic residues of Src mediate membrane binding through electrostatic interaction with acidic phospholipids. *Proc Natl Acad Sci USA* 91, 12253–12257.
- Simons K, Toomre D (2000). Lipid rafts and signal transduction. *Nat Rev Mol Cell Biol* 1, 31–39.
- Song SP, Hennig A, Schubert K, Markwart R, Schmidt P, Prior IA, Bohmer FD, Rubio I (2013). Ras palmitoylation is necessary for N-Ras activation and signal propagation in growth factor signalling. *Biochem J* 454, 323–332.
- Suzuki KG, Fujiwara TK, Sanematsu F, Iino R, Edidin M, Kusumi A (2007). GPI-anchored receptor clusters transiently recruit Lyn and Ga for temporary cluster immobilization and Lyn activation: single-molecule tracking study 1. *J Cell Biol* 177, 717–730.
- Wolfenson H, Lubelski A, Regev T, Klafter J, Henis YI, Geiger B (2009). A role for the juxtamembrane cytoplasm in the molecular dynamics of focal adhesions. *PLoS ONE* 4, e4304.
- Xu W, Harrison SC, Eck MJ (1997). Three-dimensional structure of the tyrosine kinase c-Src. *Nature* 385, 595–602.